Rapid Polymer/Gas Solution Formation for Continuous Production of Microcellular Plastics

C. B. Park*
Mem. ASME
MIT-Industry Microcellular
Plastics Consortium,
Department of Mechanical Engineering,
Massachusetts Institute of Technology,
Cambridge, MA 02139

N. P. Suh
Ralph E. and Eloise F. Cross
Professor of Manufacturing
Head and Professor
of Mechanical Engineering.
Fellow ASME
Department of Mechanical Engineering,
Massachusetts Institute of Technology,
Cambridge, MA 02139

An extrusion system that can create a polymer/gas solution rapidly for continuous processing of microcellular plastics is presented. Microcellular plastics are characterized by cell densities greater than 10^9 cells/cm^3 and fully grown cells smaller than 10 μm. Previously these microcellular structures have been produced in a batch process by saturating a polymeric material with an inert gas under high pressure followed by inducing a rapid drop in the gas solubility. The diffusion phenomena encountered in this batch processing is typically slow, resulting in long cycle times.

In order to produce microcellular plastics at industrial production rates, a means for the rapid solution formation is developed. The processing time required for completing the solution formation in the system was estimated from experimental data and the dispersive mixing theory based on an order-of-magnitude analysis. A means for promoting high bubble nucleation rates in the gas-saturated polymer via rapid heating is also discussed. The feasibility of the continuous production of microcellular plastics by the rapid polymer/gas solution formation and rapid heating was demonstrated through experiments. The paper includes not only a brief treatment of the basic science of the polymer/gas systems, but also the development of an industrially viable technology that fully utilizes the unique properties of microcellular plastics.

1 Introduction

Microcellular plastics are foamed plastics characterized by cell densities larger than 10^9 cells per cubic centimeter of unfoamed material and fully grown cells smaller than 10 μm in size. Microcellular plastics are created on the idea that the creation of a large number of bubbles, smaller than the pre-existing flaws in a polymer, can reduce the material cost without major compromises to mechanical properties [1]. Microcellular plastics have been shown to possess superior impact strength [2, 3], toughness [4], and fatigue life [5] compared with solid polymers. Because of these unique properties, one can imagine a large number of innovative applications of microcellular plastics. These include light-weight and high-strength parts, such as food containers, safety helmets, sporting equipment, structural parts in aircraft, and automotive components.

Batch processing of microcellular plastics was developed by Martini et al. [6, 7] and further improved by Cha et al. [8]. However, continuous processes have not been developed extensively. Kumar and Suh [9] developed a semicontinuous manufacturing process using a modified thermoforming process. The purpose of this paper is to present a prototype of a continuous manufacturing process for microcellular plastics with a particular emphasis on the formation of a polymer/gas solution.

2 Background on Processing of Microcellular Plastics

A typical batch process for producing microcellular plastics is as follows. First, a polymer is saturated with a high pressure gas, such as carbon dioxide or nitrogen, in a high pressure chamber. Then, the gas-saturated polymer is subjected to a rapid pressure drop and a rapid temperature increase, resulting in the nucleation and growth of billions of gas nuclei [6]. The rapid decompression and rapid heating induce a sudden drop of gas solubility in the polymer because this solubility decreases as the pressure decreases and as the temperature increases [10–13]. The sudden drop in the gas solubility (or the supersaturation) creates a thermodynamic instability in the polymer/gas solution, which is the main driving force for nucleation of microvoids.

Figure 1 shows the morphology change of polymer and gas systems in the batch process. Initially, the gas and polymer were separate systems and through diffusion they become a single-phase solution. Then, a thermodynamic instability is induced by creating a supersaturation condition in the polymer/gas solution to promote microcell nucleation. The formation of polymer/gas solution and microcell nucleation are critical steps of microcellular processing. In order to make use of a thermodynamic instability in a continuous process, these two central steps should be integrated into a single process. As a case study, this paper considers a single-screw extrusion process.

The diffusion phenomena encountered in microcellular processing is typically slow, resulting in long cycle times. Thus a critical step in continuous microcellular plastics processing is the creation of polymer/gas solutions at industrial production rates. The basic approach taken in this study to develop a rapid solution formation system is to utilize a convective diffusion for enhancing the gas diffusion rate in the polymer matrix.

3 Design of an Overall Microcellular Extrusion Process

The axiomatic approach to design [14] is used for the design of an overall microcellular extrusion process. Axiomatic design is a design guide that relies on the use of design axioms to

Copyright © 1996 by ASME
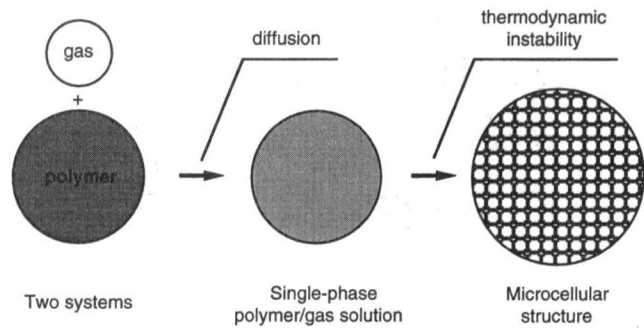
Fig. 1 Morphology change of gas and polymer systems in overall micro-cellular foaming process

Fig. 2 Schematic of an extrusion system for continuous microcellular processing

guarantee a good design. The functional requirements considered in this paper for developing a continuous microcellular process are threefold. The first is to plasticate the polymer. The second is to create a polymer/gas solution at a rate appropriate for industrial production. The third is to promote a high rate of bubble nucleation in the polymer/gas solution. The design parameters for satisfying these functional requirements are as follows: a device for polymer plastication; a device for enhancing the mass transfer of gas through diffusion; and a means of rapidly inducing a thermodynamic instability.

The design can be conveniently represented using a vector/matrix equation presented by Suh [14]. The design equation for the overall process is given by

$$
\begin{bmatrix}
\text{Plastication} \\
\text{Solution formation} \\
\text{Microcell nucleation}
\end{bmatrix}
$$
$$
= \begin{bmatrix}
X & 0 & 0 \\
X & X & 0 \\
X & 0 & X
\end{bmatrix}
\begin{bmatrix}
\text{plasticating screw motion} \\
\text{mass transfer by diffusion} \\
\text{thermodynamic instability}
\end{bmatrix} \quad (1)
$$

where X in the matrix means that there is a strong relationship between the respective functional requirement and design parameter, and 0 means that there is a weak or no relationship. For example, the gas diffusion device and the thermodynamic instability do not affect the plastication because the polymer is completely plasticated by the screw motion before the plasticated polymer melt gets to the diffusion device and the nucleation device. It should be noted that the gas is delivered to the polymer only after the polymer is completely plasticated. The plasticating screw in the extruder affects the solution formation because the screw motion generates a shear field and the mass transfer of gas through diffusion in the polymer melt is enhanced by the convective flow. However, the solution formation is not affected by the thermodynamic instability. The plasticating
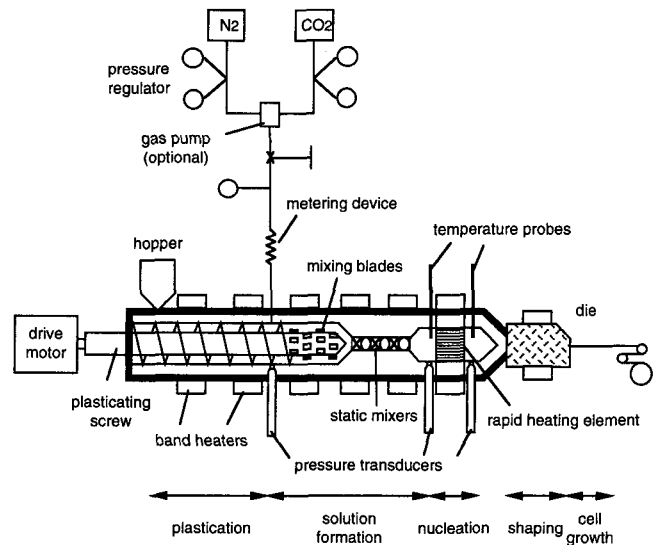
screw in the extruder affects the microcell nucleation because the screw speed affects the processing temperature [15] and the nucleation device in this work utilizes a rapid temperature increase (Section 5). The diffusion device does not affect the microcell nucleation when the polymer/gas solution is properly formed with no potential nucleation sites left in the form of voids. According to these observations, the design matrix in Eq. (1) is triangular, and therefore, the process is decoupled.

An extrusion process based on the functional requirements and the chosen design parameters is shown in Fig. 2. First, the plastication of the polymer takes place in the extrusion barrel. Then, a metered amount of gas is delivered to the polymer melt stream. The polymer/gas mixture becomes a single-phase solution in the diffusion enhancing device. Finally, a microcellular structure with a large cell density is produced when the polymer/gas solution experiences a thermodynamic instability in a rapid-heating nucleation device. In this study, a simple filament die was chosen to simplify the shaping and cell growth stages.

4 Formation of a Single-Phase Polymer/Gas Solution

One of the most critical steps in the continuous production of microcellular plastics is the formation of a polymer/gas solution at industrial production rates. When a metered amount of gas is delivered to the polymer melt stream, a two-phase polymer/gas mixture is firstly formed. Then, the large injected gas

──────── **Nomenclature** ────────

A = interfacial area of gas bubbles and polymer melt matrix, m^2
b = screw channel depth, m
D = diffusivity, cm^2/s
D_0 = diffusivity constant, cm^2/s
d_b = unstretched diameter of disintegrated bubbles, m
d_{max} = maximum length of elongated bubbles in the shear field, m
l_d = diffusion distance, m
R = universal gas constant = 8.314 J/mol-K

r_s = radius of the screw, m
s = striation thickness, m
T = temperature, K
t_d = diffusion time, s
u = linear speed of the tip of the screw flight, m/s
V = total volume of polymer melt and gas bubbles, m^3
We = Weber number
ΔE_D = activation energy for diffusion of gas in a polymer, J/mol

Φ_v = volume fraction of gas in the mixture
γ_g = mean stretching ratio of the gas bubbles
$\dot{\gamma}$ = shear rate in mixer, s^{-1}
η_g = dynamic viscosity of gas, Pa-s
η_p = dynamic viscosity of polymer matrix, Pa-s
σ = surface tension, N/m
Ω = rotational speed of the screw, min^{-1}

Table 1 Estimated gas diffusivity in polymers at elevated temperatures

polymer	D of CO_2 (cm^2/sec)		D of N_2 (cm^2/sec)	
	at 188 °C *	at 200 °C †	at 188 °C *	at 200 °C †
PS	-	1.3×10^{-5}	-	1.5×10^{-5}
PP	4.2×10^{-5}	-	3.5×10^{-5}	-
PET	-	2.6×10^{-6}	-	8.8×10^{-7}
HDPE	5.7×10^{-5}	2.4×10^{-5}	6.0×10^{-5}	2.5×10^{-5}
LDPE	-	1.1×10^{-4}	-	1.5×10^{-4}
PTFE	-	7.0×10^{-6}	-	8.3×10^{-6}
PVC	-	3.8×10^{-5}	-	4.3×10^{-5}

*   Durril and Griskey [11]
†   Van Krevelen [12]

bubbles are broken into smaller bubbles and stretched through shear mixing. Eventually, the gas diffuses into the polymer matrix, forming a single-phase solution.

Diffusion of gas in a polymer is known to be very slow. For example, let us calculate the time required for a gas to diffuse to a depth of 1 mm. As an order of magnitude, the diffusion distance (l_D) can be estimated as

$$l_d \approx \sqrt{Dt_d} \qquad (2)$$

The diffusivity of CO_2 in most thermoplastics at room temperature is approximately 5×10^{-8} cm^2/sec [12]. Therefore, the diffusion time (t_d) is estimated as

$$t_d \approx l_d^2/D \approx 200{,}000 \text{ s} \approx 55 \text{ h} \qquad (3)$$

This diffusion time is too long to be industrially applicable. In order to achieve industrial production rates for the solution formation, a technique for enhancing diffusion needs to be developed. The basic strategies for fast solution formation are to raise the diffusivity by increasing the temperature and to reduce the diffusion distance through convective diffusion.

4.1 Estimation of Gas Diffusivity in Polymers at Elevated Temperatures.

In general, the diffusivity of gas in a polymer changes with temperature, pressure, and gas concentration [10–12, 16] and can be approximated as

$$D = D_0 \exp(-\Delta E_D/RT) \qquad (4)$$

In this expression, the effect of the concentration dependence on the diffusivity is neglected. Since the diffusivity increases as temperature increases, the rate of gas diffusion is enhanced by processing the mixture at a high temperature. Therefore, compared to room temperature, the gas diffusion rate for the polymer mixture is increased in the heated extrusion barrel.

Only limited data is available for gas diffusion in polymers at high temperatures [10–12]. The estimated diffusivities are summarized in Table 1. At 200°C, a typical diffusivity of CO_2 and N_2 in a thermoplastic is approximately 10^{-6} cm^2/sec.

4.2 Convective Diffusion: Mixing and Diffusion.

In order to design a rapid solution formation device, the critical process parameters of solution formation needs to be identified. In this section, the physical phenomena behind a continuous solution formation process is qualitatively analyzed and a model for predicting the required processing time for the solution formation is developed.

Mass transfer by molecular diffusion is analogous to heat transfer because the heat conduction and diffusion equations have the same form [17]. Just as the heat transfer rate is enhanced by convection, the diffusion rate is also enhanced by convection. Convection brings low gas concentration polymer into contact with high gas concentration bubbles. This convective flow induces a high concentration gradient which promotes diffusion.

The concentration profile in diffusion is similar to the temperature profile in heat transfer associated with a similar heat source. Therefore, when the diffusion source is stationary and exhibits a simple shape, such as a flat plate, the concentration profile may be expressed from known heat transfer solutions with an appropriate change in notation. When the diffusion source is also moving, the analysis of the problem becomes complicated. In investigating the local concentration profile, the first step is to trace the shape of the source boundary. Since the diffusion sources in this study are the gas bubbles which are moving along the polymer melt, the dynamic behavior of the gas bubbles and the polymer melt should be investigated first. The diffusion phenomena will then be analyzed based on the mixing behavior of the gas bubbles and the polymer melt.

As the gas molecules diffuse into the polymer matrix, the total volume of the gaseous phase diminishes in size until the gas completely dissolves into the matrix. Since the size of one phase component is changing, the mixing behavior of the two-phase mixture is far more complicated than simple mixing. It is very difficult to investigate the mixing behavior of the two-phase mixture and the flow fields of each phase. Since the diffusion phenomenon strongly depends on mixing behavior, the analysis of the mass transfer phenomena of diffusion is also complicated. Therefore, the diffusion of gas into the polymer matrix may not be completely analyzed.

Despite the complication of modeling the dynamic behavior of the mixture of the two fluids, the diffusion rate is greatly enhanced when the diffusion source is also moving. As the degree of mixing increases, more polymer melt is brought into contact with the source of the high gas concentration which increases the effect of convective diffusion. This convective diffusion effect is enhanced through an increase in the interfacial area per unit volume, a reduction of the diffusion distance, and a redistribution of the local gas concentration profile in the polymer matrix. In addition, since the diffusion rate strongly depends on the mixing behavior, the diffusion time can be controlled by varying the degree of mixing.

The concept of convective diffusion can be effectively utilized to enhance the diffusion rate in an extrusion barrel. One technique for rapid solution formation using convective diffusion employs laminar mixing in the molten polymer shear field. Since the mixing accomplished by the simple screw motion is limited, efforts were also made to enhance the mixing effectiveness by introducing various mixing sections in the extruder [18, 19]. The idea behind the mixing sections is that reorientation of the mixture during processing will enhance the effectiveness of shear mixing. Using the mixing sections, the diffusion time would decrease due to the enhanced degree of mixing.

The shearing/wiping action of the extrusion screw draws gas streams/bubbles into the molten polymer shear field. The mixing action of the shear field slowly disperses the source of high gas concentration (i.e., the gas streams/bubbles) into the polymer matrix. The gas eventually diffuses into the polymer and a single-phase solution is formed. The convective diffusion effect in the shear field generated by the screw motion is well described for the devolitilization of polymer solution in a twin-screw extruder [20, 21]. The deformation and movement of the concentration source and the diminishing of the total volume of the gaseous phase component causes the analyses of the mixing behavior of the two-phase mixture and the diffusion phenomena to be very difficult. However, we can still estimate the diffusion time for completing the solution formation based on the estimated striation thickness of the gas and polymer mixture.
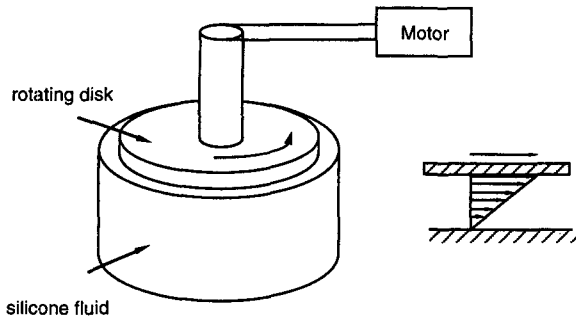
Fig. 3 Experimental apparatus for generating a simple shear field

As an order of magnitude, the diffusion time can be estimated as the time at which the diffusion distance is of the same order as the striation thickness of the mixture (s):

$$t_d \approx l_d^2/D \approx s^2/D \qquad (5)$$

For example, if the striation thickness is 100 μm, the diffusion time would be 100 seconds for a typical diffusivity of 10^{-6} cm^2/s at 200°C.

Because the diffusion rate strongly depends on the degree of mixing, the mixing behavior of the gas and polymer melt is investigated. The mixing theory of highly viscous fluids describes the growth of interfacial areas in different types of shear flows. The interfacial area (A) per unit volume is a key measure of mixing [22]. Related to this interfacial area per unit volume is the striation thickness which is defined as the average distance between similar interfaces of the components in the mixture. These two parameters representing the degree of mixing are related by the expression [23]:

$$s = 2V/A \qquad (6)$$

where V is the total volume of the polymer melt matrix and gas bubbles. From Eq. (6), the striation thickness as a function of stretching can be expressed as [24, 25]

$$s \approx d_b/\Phi_v\gamma_g \qquad (7)$$

Therefore, the disintegrated bubble size (d_b), the volume fraction of gas (Φ_v), and the mean stretching ratio of bubbles (γ_g) should be estimated in order to estimate the striation thickness. For a typical solubility of 10% at 200°C and 27.6 MPa (4000 psi) [11, 12], the volume fraction of CO_2 in the mixture is calculated to be 0.22 [26]. The disintegrated bubble size and the mean stretching ratio are estimated in the following paragraphs.

The mixing behavior of a gas in a polymer melt follows the dispersive mixing theory [27, 28]. This theory states that the minor components, gas bubbles in the present case, are stretched by the shear forces and disintegration of the bubbles takes place when the stretching exceeds a critical value of the Weber number [29–31]. The Weber number (We) is defined as

$$\text{We} = \frac{\dot{\gamma} d_b\eta_p f(\eta_g, \eta_p)}{2\sigma} = \frac{\text{shear forces}}{\text{surface forces}} \qquad (8)$$

where

$$f(\eta_g, \eta_p) = \frac{[19(\eta_g/\eta_p) + 16]}{[16(\eta_g/\eta_p) + 16]} \qquad (9)$$

It should be noted that the shear force to surface force ratio is also known as the capillary number [21, 32]. For typical values of η_p and η_g [33], the disintegrated bubble diameter can be estimated as follows:

$$\eta_p = 2 \times 10^2 \text{ Pa-s}$$

$$\eta_g = 3 \times 10^{-5} \text{ Pa-s}$$

$$\eta_g/\eta_p = 1.5 \times 10^{-7} \qquad (10)$$

$$f(\eta_g, \eta_p) = 1 \qquad (11)$$

The critical Weber number for the viscosity ratio of 1.5×10^{-7} in a simple shear field is estimated as We $\approx$ 300 [34].

The surface tension of polystyrene at 200°C is [35]

$$\sigma = 40.7 - 0.072 \, (T - 293)$$

$$= 28 \text{ dyne/cm} = 0.028 \text{ N/m} \qquad (12)$$

The shear strain rate in an extrusion barrel for the screw RPM (Ω) of 90 min^{-1} and the screw channel depth (b) of 0.8 mm is estimated as

$$\dot{\gamma} \approx u/b = r_s(2\pi\Omega/60)/b$$

$$= 8.7 \text{ mm } (2\pi \times 90/60) \text{ s}^{-1}/0.8 \text{ mm} \approx 100 \text{ s}^{-1} \qquad (13)$$

Finally, the disintegrated bubble size is determined as

$$d_b = 2\sigma\text{We}/[\dot{\gamma}\eta_p f(\eta_g, \eta_p)] = 8.4 \times 10^{-4} \text{ m} \approx 1 \text{ mm} \qquad (14)$$

Therefore, when the gas is injected into the extrusion barrel, the large injected bubbles are stretched and disintegrated into 1 mm diameter bubbles in the shear field generated by the screw.

Now let us estimate the bubble stretching ratio. In order to estimate the bubble stretching ratio in the shear field of the extrusion barrel, an experimental apparatus which generates a simple shear field was used as shown in Fig. 3. The stretching behavior of a 1 mm diameter air bubble in silicone fluids (Dow Corning #200 Fluids) was investigated. The rotating disk and the container are transparent so that the stretching behavior of the air bubble can be observed.

The bubble stretching ratio (γ_g) is defined as

$$\gamma_g = d_{\max}/d_b \qquad (15)$$

where $d_{\max}$ is the maximum length of the elongated bubble in the shear field as shown in Fig. 4. The bubble stretching ratio was measured at various shear strain rates of the silicone fluid bath. The bubble was not stretched proportionally to the total shear strain/deformation of the silicone fluid bath. Instead, the bubble maintained a stretched shape at the steady state as the silicone matrix was being sheared at a certain rate. This implies that the mixing of gas and polymer does not follow the distributive mixing theory. This theory states that the minor component follows the streamlines of the matrix fluid (major component) and that the distribution depends on the total deformation of the system [28, 36]. In fact, the mixing behavior of the polymer/gas system follows the dispersion mixing theory as discussed above.

The bubble stretching ratio was measured at various shear strain rates of the silicone matrix. According to the experimental results, the maximum length of the stretched bubble, i.e., the bubble stretching ratio, increased as the shear strain rate of the silicone matrix increased. The bubble stretching ratio was also affected by the viscosity of the silicone fluid. Two different viscosity fluids of 600 Pa-s and 10 Pa-s were used in the experi-
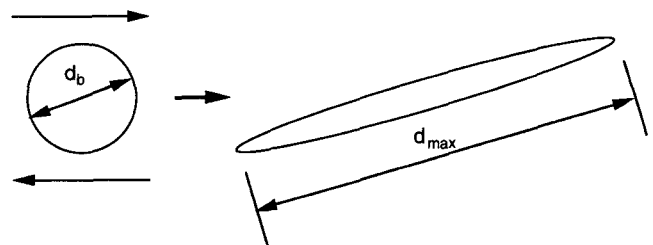

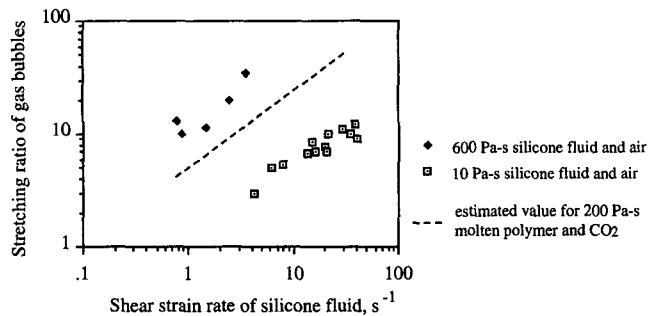**Fig. 4 Stretching behavior of a gas bubble in a shear field**

Fig. 5 Stretching ratio of 1 mm diameter air bubbles in silicone fluid baths

ments. Higher bubble stretching ratios were observed in the higher viscosity fluid for the same stretching rates. The measured bubble stretching ratios at various shear strain rates for the two viscosity fluids are plotted in Fig. 5. For a typical polymer matrix viscosity of $\eta_p = 200$ Pa-s, the bubble stretching ratio is estimated to be about 100 for the equivalent shear rate of 100 s^{-1} in the extrusion.

From Eq. (7), the striation thickness is estimated as

$$s \approx d_b/\Phi_v\gamma_g \approx 1 \text{ mm}/(0.22 \times 100) = 45 \ \mu\text{m} \qquad (16)$$

It may be noted that the striation thickness of the gas and polymer in this system is two orders of magnitude larger than a typical striation thickness for similar polymers in a 30 mm single-screw extruder [37]. Based on this striation thickness, the required diffusion time is estimated to be

$$t_d \approx s^2/D \approx (45 \times 10^{-4})^2/1 \times 10^{-6} = 20 \text{ s} \qquad (17)$$

The order-of-magnitude analysis shown above predicts that the solution formation will be completed in 20 seconds when the polymer/gas system is fully mixed and the striation thickness is 45 μm. Therefore, the continuous solution formation can be achieved in extrusion systems without substantially decreasing the processing rates from normal industrial rates.

It should be emphasized that the model described above to predict the required processing time for the continuous solution formation is developed based on an order-of-magnitude analysis. The stretching ratio of the gas bubbles in a polymer melt was estimated based on the stretching behavior of the air bubbles in silicone fluids. It is expected that a significant amount of error is involved in this estimation. In addition, due to the limited available gas diffusivity data for high concentration at elevated temperatures, the concentration-dependent nature of the diffusivity could not be accounted for in this order-of-magnitude analysis. In order to develop a better model of the continuous formation of a single-phase polymer/gas solution, fundamental research on the diffusivity of gas at elevated temperatures and pressures, and the polymer/gas mixing behavior in the mixing elements should be carried out.

5 Design of Nucleation Device: Rapid Heating Element

The next critical step in the continuous production of microcellular plastics is to promote a high rate of bubble nucleation in the polymer/gas solution. The nucleation of bubbles is the transformation of small clusters of gas molecules into energetically stable pockets of molecules with distinct cell walls. The microcellular process requires that the nucleation cell density be larger than 10^9 cells/cm^3 corresponding to a fully grown cell size less than 10 μm. The key to producing the required cell density is achieving a very high rate of cell nucleation in the polymer/gas solution.

High nucleation rates have been achieved in batch processes using the thermodynamic instability induced by creating a supersaturation condition in the polymer/gas system. In order to make use of a thermodynamic instability in a continuous process, a rapid drop in the gas solubility must be induced in the polymer/gas solution. Since the solubility of gas in a polymer changes with temperature and pressure, a thermodynamic instability can be induced by rapidly varying the temperature or pressure.

Since the solubility of a gas in a polymer decreases as the temperature increases, a high cell nucleation rate can result when the polymer/gas solution is heated rapidly. An effective heating element for polymers has been designed by Park and Suh [38]. The heating element, comprised of small tubes and a band heater as shown in Fig. 6, is designed to increase the temperature of the flowing polymer by 50°C/s.

6 Experiments

6.1 Experimental Set-up. Based on the proposed design, an experimental extrusion set-up was prepared (the schematic is shown in Fig. 2). The extruder used is a Brabender Type 2523-$\frac{3}{4}$ inch extruder with a simple filament die. The barrel was tapped near the end of the plasticating screw and was connected to a high pressure gas cylinder of CO_2 and N_2. A mixing screw (Brabender 05-00-051) and a six element static mixer of diameter 6.8 mm were used for enhancing the mixing of gas and polymer melt.

Seven band heaters and temperature controllers were installed: three for the extrusion barrel, two for the static mixers, one for the rapid heating device, and one for the die. Two thermocouples were installed: one located upstream and one downstream of the heating element, to measure the temperature rise in the polymer. Three pressure transducers were also installed: one to measure the pressure of the extrusion barrel where the gas is injected, one at the end of the mixing/diffusion device to measure the pressure of the solution formation process and one downstream from the heating element to measure the pressure drop across the heating element.

6.2 Experiments and Results. Several materials, including semicrystalline and amorphous polymers, were processed with CO_2 and N_2. The polymers used in the experiment were Phillips 66 Marlex Polypropylene (PP), Monsanto 3350 High Impact Polystyrene (HIPS), and GE Cycolac Acrylonitrile Butadiene Styrene (ABS).

The temperature rise of most polymers induced by the heating element was about 40°C. The extruded samples were examined by a scanning electron microscope (SEM) to characterize the microstructures. Figures 7(a) and (b) show the SEM pictures of the extruded PP. When processed with N_2 and CO_2, the cell densities were 3×10^7/cm^3 and 6×10^8 cells/cm^3, respectively. Figures 8(a) and (b) show the SEM pictures of the extruded HIPS. The cell densities were 9×10^7 cells/cm^3 and 8×10^9 cells/cm^3 for N_2 and CO_2 injection, respectively. Figure 9 shows
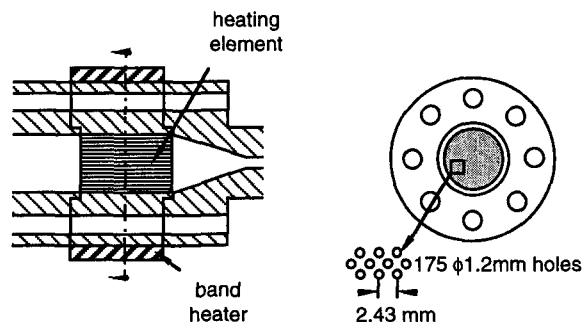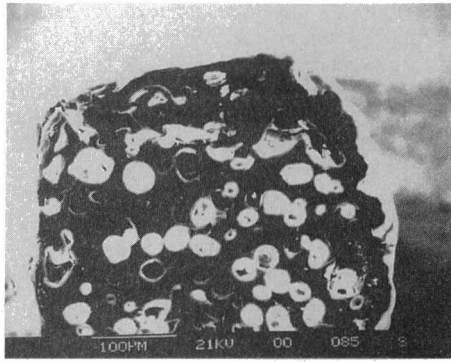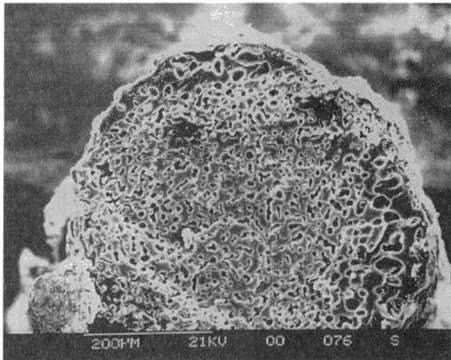

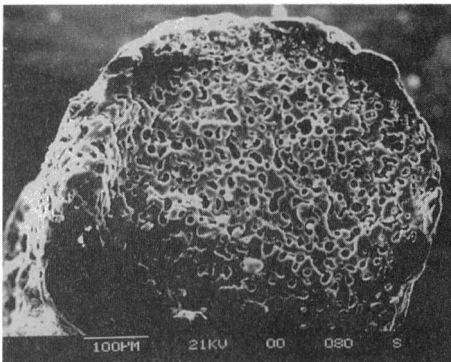Fig. 6 Rapid heating element for microcell nucleation
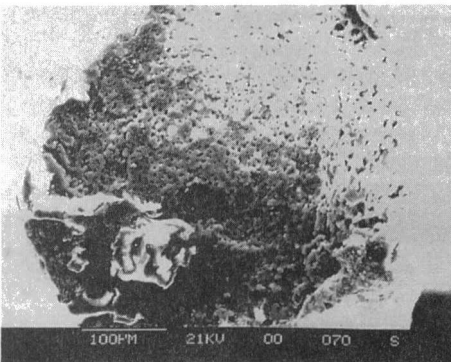
(a) N₂ Injection

(b) CO₂ Injection

Fig. 7   Scanning electron micrographs of extruded PP

(a) N₂ injection

(b) CO₂ injection

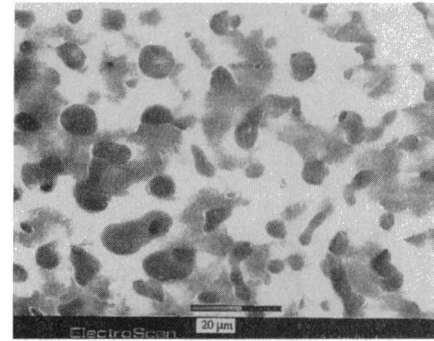Fig. 8   Scanning electron micrographs of extruded HIPS

Fig. 9   Scanning electron micrograph of extruded ABS (CO_2 injection)

the SEM picture of the extruded ABS. When CO_2 was processed, the cell density was $9 \times 10^8/cm^3$. The results are summarized in Table 2.

6.3 Discussion. The thermodynamic instability induced from the rapid formation of a polymer/gas solution and the rapid heating seemed sufficient since a large number of cells were nucleated. About $10^8 - 10^{10}$ nucleated cells per cubic cm of unfoamed material were found in the processed samples of PP, HIPS, and ABS when CO_2 was processed. However, when N_2 was processed, $10^7 - 10^8$ cells/cm^3 were found in the PP and HIPS samples. The lower cell densities seem to be due to the lower solubility of N_2 in the polymers [10–12]. The amount of gas dissolved in the polymer directly affects the cell density because a greater thermodynamic instability will be induced when the polymer has more dissolved gas.

The degree of mixing of the gas and the polymer melt is also very important because it determines the diffusion time for the formation of the polymer/gas solution. When the gas and the polymer melt are not mixed well, the gas does not completely dissolve into the polymer matrix during the given processing time. The residual gas voids then affect the cell density because the existence of these voids prohibits the formation of potential nucleation sites [7] and results in nonuniform cell sizes. For example, when the plasticating screw speed fell below 35 RPM in the processing of HIPS with CO_2, the cell density was about 10^6 cells/cm^3, and large cavities were observed in the samples.

The critical parameters in the developed extrusion system for continuous formation of a single-phase solution are the dissolved gas amount, the degree of mixing, the processing pressure, the processing temperature, and the processing time. In order to better understand the solution formation process in the extrusion system, fundamental study on the diffusivity of gas at high temperatures and pressures, and the polymer/gas mixing behavior in the mixing sections should be conducted as discussed earlier.

Since the processing of microcellular plastics does not use CFCs, but rather inert gases such as CO_2 and N_2, the process of the polymer/gas solution formation and microcell nucleation described in this paper could be utilized for replacing CFCs in

Table 2   Experimental results

Polymer	Cell Density	
	CO₂ Injection	N₂ Injection
PP	6×10^8 cells/cm^3	3×10^7 cells/cm^3
HIPS	8×10^9 cells/cm^3	9×10^7 cells/cm^3
ABS	9×10^8 cells/cm^3	-

conventional foaming processes. The process developed in this research can also be applied to other types of continuous processes such as sheet extrusion and injection molding.

7 Concluding Remarks

In this paper, a continuous process of microcellular plastics by rapid formation of a polymer/gas solution and rapid heating is presented. Previously microcellular structures have been produced in batch processes by exposing a polymeric material to a high pressure gas for a long time to saturate the polymer with gas and by inducing a rapid drop in the gas solubility. However, the time required for the solution formation in batch processes is too long to be industrially applicable. In order to produce microcellular plastics at industrial production rates, a means for the rapid solution formation needs to be developed. The basic strategies for fast solution formation are to raise the diffusivity by increasing the temperature and to reduce the diffusion distance through convective diffusion.

An extrusion system that can create a polymer/gas solution without substantially decreasing the processing rates from normal industrial rates was developed based on these strategies. First, polymer pellets are plasticated by the motion of the plasticating screw in an extrusion barrel. Then, a metered amount of gas is injected into the polymer melt. The large gas bubbles entrained in the polymer flow are broken into smaller bubbles by the shearing action of the screw. Further mixing is accomplished through the irregular mixing blades on the screw as well as the static mixers. With the aids of convective diffusion promoted in the mixing sections, a single-phase polymer/gas solution can be formed rapidly.

Research efforts were also directed toward understanding the major physics behind the developed solution formation system. The deformation and movement of the concentration source (i.e., gas bubbles) and the diminishing of the total volume of the gaseous phase component caused the analyses of the mixing behavior of the two-phase mixture and the diffusion phenomena to be very difficult. However, the processing time required for the solution formation could be estimated from experimental data and the dispersive mixing theory based on an order-of-magnitude analysis. The diffusivities of CO_2 and N_2 at elevated temperatures and pressures were estimated from the published data.

A means for promoting high bubble nucleation rates in the gas-saturated polymer via rapid heating was also presented. The concept of polymer/gas solution formation and microcell nucleation by rapid heating was examined through experimental work. About 10^8–10^{10} cells/cm^3 were nucleated when PP, HIPS, and ABS were processed with CO_2. Relatively low cell densities of 10^7–10^8 cells/cm^3 were found in the samples of PP and HIPS when N_2 was injected into the polymer melt. These experiments demonstrated the feasibility of the continuous production of microcellular plastics by the rapid polymer/gas solution formation and a rapid solubility drop.

Acknowledgment

References

1 Suh, N. P., 1980, Private Communication, MIT-Industry Polymer Processing Program.

2 Waldman, F. A., 1982, "The Processing of Microcellular Foam," S.M. Thesis, Massachusetts Institute of Technology, Cambridge, MA.

3 Collias, D. I., Baird, D. G., and Borggreve, R. J. M., 1994, "Impact Toughening of Polycarbonate by Microcellular Foaming," *Polymer*, Vol. 25, No. 18, pp. 3978–3983.

4 Baldwin, D. F., and Suh, N. P., 1992, "Microcellular Poly(ethylene terephthalate) and Crystallizable Poly(ethylene terephthalate)," *Proceedings of the SPE-ANTEC '92*, Vol. 38, pp. 1503–1507.

5 Seeler, K. A., and Kumar, V., 1993, "Tension-Tension Fatigue of Microcellular Polycarbonate: Initial Results," *Journal of Reinforced Plastics and Composites*, Vol. 12, No. 3, pp. 359–376.

6 Martini, J., Suh, N. P., and Waldman, F. A., 1984, "Microcellular Closed Cell Foams and Their Method of Manufacture," *U.S. Patent 4473665*.

7 Martini, J., 1981, "The Production and Analysis of Microcellular Foam," S.M. Thesis, Massachusetts Institute of Technology, Cambridge, MA.

8 Cha, S. W., Suh, N. P., Baldwin, D. F., and Park, C. B., 1992, "Microcellular Thermoplastic Foamed with Supercritical Fluid," *U.S. Patent 5158986*.

9 Kumar, V., and Suh, N. P., 1990, "A Process for Making Microcellular Thermoplastic Parts," *Polym. Eng. Sci.*, Vol. 30, No. 20, pp. 1323–1329.

10 Newitt, D. M., and Weale, K. E., 1948, "Solution and Diffusion of Gases in Polystyrene at High Pressures," *J. of Chem. Sci.*, pp. 1541–1549.

11 Durril, P. L., and Griskey, R. G., 1969, "Diffusion and Solution of Gases in Thermally Softened or Molten Polymers: Part II," *A.I.Ch.E. Journal*, Vol. 15, No. 1, pp. 106–110.

12 Van Krevelen, D. W., 1976, *Properties of Polymers*, Elsevier, New York, pp. 404–425.

13 Vieth, W. R., Tam, P. M., and Michaels, A. S., 1966, *Journal of Colloid and Interface Science*, Vol. 22, pp. 360–370.

14 Suh, N. P., 1990, *The Principles of Design*, Oxford University Press.

15 Lindt, J. T., 1976, "A Dynamic Melting Model for a Single-Screw Extruder," *Polymer Engineering and Science*, Vol. 16, No. 4, pp. 284–291.

16 Koros, W. J., and Paul, D. R., 1980, "Sorption and Transport of CO_2 above and below the Glass Transition of Poly(Ethylene Terephthalate)," *Polym. Eng. Sci.*, Vol. 20, No. 1, pp. 14–19.

17 Bird, R. B., Stewart, W. E., and Lightfoot, E. N., 1960, Transport Phenomena, pp. 597–625 and 642–652.

18 Erwin, L., 1978, "Theory of Mixing Sections in Single Screw Extruders," *Polym. Eng. Sci.*, Vol. 18, No. 7, pp. 572–576.

19 Raunwendaal, C., 1991, "Mixing in the Single-Screw Extruders," In: *Mixing in Polymer Processing*, Chris Raunwendaal, ed., Marcel Dekker, Inc., pp. 129–240.

20 Foster, R. W., and Lindt, J. T., 1990, "Bubble-Free Devolatilization in Counterrotating Nonintermeshing Twin-Screw Extruder," *Polymer Engineering and Science*, Vol. 30, No. 7, pp. 424–430.

21 Foster, R. W., and Lindt, J. T., 1990, "Twin Screw Devolatilization: From Foam to Bubble Free Mass Transfer," *Polymer Engineering and Science*, Vol. 30, No. 7, pp. 621–634.

22 Spencer, R. S., and Willy, R. M., 1949, "The Mixing of Very Viscous Liquids," *Journal of Colloid Science*, Vol. 6, pp. 133–145.

23 Schrenk, W. J., Cleereman, K. J., and Alfrey, T., 1963, "Continuous Mixing of Very Viscous Fluids in an Annular Channel," *SPE Transactions*, Vol. 3, pp. 192–200.

24 Mohr, W. D., Saxton, R. L., and Jepson, C. H., 1957, "Mixing in Laminar-flow Systems," *Industrial and Engineering Chemistry*, Vol. 49, No. 11, pp. 1855–1862.

25 Kim, V. S., Skachkov, V. V., and Koshelev, G. G., 1972, "Analysis of Mixing Processes in the Screw Chaneels of a Single-screw Extruder during Processing of Polymer Mixtures," *Plaste Kautschuk*, Vol. 19, No. 2, pp. 128–134.

26 IUPAC, 1973, *International Thermodynamic Tables of the Fluid State 3-Carbon Dioxide*, Pergamon Press.

27 Bolen, W. R., and Colwell, R. E., 1958, "Intensive Mixing," *SPE Journal*, Vol. 14, No. 8, p. 24.

28 Tadmor, Z., and Gogos, C. G., 1976, *Principles of Polymer Processing*, Wiley Int.

29 Taylor, G. I., 1934, "The Formation of Emulsions in Definable Fields of Flow," *Proceedings of the Royal Society of London*, Series A, Vol. 146, pp. 501–523.

30 Rumscheidt, F. D., and Mason, S. G., 1961, "Particle Motions in Sheared Suspensions," *Journal of Colloid Science*, Vol. 16, pp. 238–261.

31 Mutsakis, M., Streiff, F. A., and Schneider, G., 1986, "Advances in Static Mixing Technology," *A.I.Ch.E., Chemical Engineering Program*, pp. 42–48.

32 Khan, S. A., and Armstrong, R. C., 1987, "Rheology of Foams: II. Effects of Polydispersity and Liquid Viscosity for Foams Having Gas Fraction Approaching Unity," *Journal of Non-Newtonian Fluid Mechanics*, Vol. 25, pp. 61–92.

33 Vukalovich, M. P., and Altunin, V. V., 1968, *Thermophysical Properties of Carbon Dioxide*, translated by Collet's Ltd., pp. 383–423.

34 Karam, H. J., and Bellinger, J. C., 1968, "Deformation and Breakup of Liquid Droplets in a Simple Shear Field," *Industrial and Engineering Chemistry, Fundamentals*, Vol. 7, pp. 576–581.

35 Wu, S., 1982, *Polymer Interface and Adhesion*, Marcel Dekker, pp. 67–132.

36 Nakajima, N., and Harrell, E. R., 1984, "Contributions of Elastomer Behavior to Mechanisms of Carbon Black Dispersion," *Rubber Chemistry and Technology*, Vol. 57, pp. 153–167.

37 Ghosh, A. K., Ranganathan, S., Lindt, J. T., and Lorek, S., "Blend Morphology Development in a Single Screw Extruder," *Proceedings of the SPE-ANTEC '91*, Vol. 37, pp. 232–236.

38 Park, C. B., and Suh, N. P., 1992, "Rapid Heating for Microcellular Nucleation in a Polymer Melt," *Proceedings of the SPE-ANTEC '92*, Vol. 38, pp. 1513–1518.